Simulating the behaviour of folded cartons during complex packing operations

D M Sirkett*, **B J Hicks, C Berry, G Mullineux,** and **A J Medland**
Innovative Manufacturing Research Centre, Department of Mechanical Engineering, University of Bath, Bath, UK

The manuscript was received on 27 June 2005 and was accepted after revision for publication on 6 July 2006.

DOI: 10.1243/0954406JMES109

Abstract: The folding carton is a widely used packaging solution. Recent European Union packaging legislation has forced carton manufacturers to use lighter-weight grades of carton board. This typically results in a reduction in board stiffness, which can lead to decreased process efficacy or even prevent successful processing. In order to overcome this, end-users lower production rates and fine-tune packaging machine settings for each pack and material. This trial-and-error approach is necessary because the rules relating machine set-up to pack design and material properties are not generally well known. The present study addresses this fundamental issue through the creation of a finite-element computer simulation of carton processing. Mechanical testing was performed to ascertain the key mechanical properties of the carton walls and creases. The carton model was validated against the experimental results and was then subjected to the machine–material interactions that take place during complex packaging operations. The overall approach was validated and the simulation showed good agreement with the physical system. The results of the simulation can be used to determine guidelines relating machine set-up criteria to carton properties. This will improve responsiveness to change and will ultimately allow end-users to process thinner lighter-weight materials more effectively.

Keywords: packaging machine design, finite-element analysis, carton board, carton erection

1 INTRODUCTION

Packaging is vitally important for the consumer goods industry. It serves to protect and contain the contents during transit and storage, and upon arrival at the retailer, it provides tamper evidence. Its external appearance can help sell the product and also provides information about the contents.

The European packaging industry is valued at £86.8 billion, of which 11 per cent is accounted for by the UK [**1**]. Of the 74.1 million tonnes of packaging consumed annually in Europe, the largest sector is paper and board, which accounts for 43 per cent of this total [**1**]. Within this sector, one of the most widely used packaging solutions is the folding carton. The folding carton industry in Europe has a turnover of £4.5 billion and employs around 57 000 workers [**2**]. The annual consumption of folding cartons in Europe is 4.5 million tonnes [**2**], of which 13.7 per cent is accounted for by the UK at a value of £1.0 billion [**3**].

Recent European Union (EU) legislation has specified targets for the reduction of packaging waste and increased materials recovery and recycling throughout the packaging industry. By December 2008, member states are obliged to recycle a minimum of 55 per cent by weight of all packaging waste and to increase the proportion of recycled material in paper-based packaging for food to at least 60 per cent by weight [**4**]. In order to comply with the new regulations, carton manufacturers are being encouraged to use thinner, lighter-weight grades of carton board and boards with a higher recycled material content. This has had a significant impact on the convertibility of prefolded, flattened cartons and has stimulated demand for a greater understanding of the processes involved.

A folding carton is manufactured from paper laminate board and is generally supplied in a prefolded, flattened state ready to be unfolded or

**Corresponding author: Innovative Manufacturing Research Centre, Department of Mechanical Engineering, University of Bath, Claverton Down, Bath BA2 7AY, UK. email: enpdms@bath.ac.uk*

'erected' at high speed immediately prior to content insertion. There are several reasons for its success. It is economical in terms of materials cost and manufacturing processes. It can be delivered to the end-user in a space-saving collapsed state. The appeal of the product can be enhanced through the use of high-quality printing on the exterior, and when the contents are finished, the carton can be returned to the flattened state to minimize the waste volume. The environmental impact of disposal is also minimal because the carton material is biodegradable.

The characteristic that allows the ease of manufacture of the folding carton is the laminar property of the board. This allows for two different states – a rigid state in which the layers composing the board are well bonded together and a flexible state in which the layers are delaminated along a fold [**5**]. Delamination is induced by initial creasing. Creases encourage the board to fold along predetermined lines without detracting from the tensile strength of the material [**6**]. This allows the board to be accurately formed into stiff, three-dimensional structures that are ideal packaging solutions.

The flexural rigidity of the board has been identified as the most important performance parameter of a rigid package [**7**], and the ratio of board stiffness to bending stiffness is the key to determine the convertibility of folding cartons [**8**]. However, thinner boards generally exhibit lower stiffness, and the impact of using recycled board on stiffness can be equivalent to a loss of $\sim$10 per cent of thickness for board used in folding cartons [**9**]. As a consequence, the behaviour of such materials during processing with present designs of packaging machines is less predictable [**10**] and this is further frustrated by a large number of materials from many different suppliers. The stage of carton manufacture where these factors have the greatest effect is the erection process.

At present, many packaging machines are designed and set up on a trial-and-error basis because the understanding necessary to relate a particular pack geometry and material to the optimum machine set-up is not well established. Machine adjustments are occasionally calibrated for a range of preselected pack sizes or types, but these settings are not necessarily optimal and there is seldom any indication of the acceptable tolerance range.

In order to remain competitive, the packaging industy, in common with all manufacturing industries today, is expected to be able to supply machinery that can deliver increased performance and accommodate wide variations in material properties and pack design. In the production of packaging machines, the ability to achieve this is frustrated by a lack of understanding of the material behaviour and the material–machine interactions that occur during processing. It has been shown in previous work [**11**, **12**] that the limiting factors often occur at the machine–material interface. One way to overcome this is to create computational tools that allow the interactions to be explored and a fundamental understanding to be developed.

Although very little work has been carried out with the purpose of investigating the machine–material interactions that take place during carton packaging, such studies have been performed for similar products. The finite-element (FE) approach has been used recently to study the brim formation process, which is the final stage in the manufacture of a paper cup [**13**], the sealing of metalized plastic pouches for packaging liquid products [**14**], and the production of plastic bottles by blow-moulding [**15**]. In these examples, the interaction of the material with the machine elements was key to the success of the operation and this reinforces the need for greater understanding of the machine–material interaction.

The work reported in this paper considers the creation of a computer-based simulation of the machine–material interactions that occur as a carton is processed within a packaging machine. In particular, this study considers the process of normal carton erection and develops a model of the behaviour of the pack during processing.

First, the paper provides an overview of the manufacture of a folding carton, describing the behaviour of the material used in its construction. Following this, the complex machine–material interactions that are considered in the present study are outlined. These are contextualized in a description of a mechanism used in a common form of packaging machine. Details of the modelling approach are provided along with a validation of the pack model in isolation. The pack model is then extended to predict its behaviour during processing in the considered packaging machine. Results of the process simulation are then compared with the high-speed video footage.

2 BACKGROUND

This section discusses the construction and key components of folded cartons. Following this is an overview of the critical factors which need to be modelled in order to simulate the behaviour of cartons during processing operations.

2.1 Production of folding cartons

As stated previously, this paper deals with carton conversion. In particular, the erection phase [Fig. 1 (c)] is considered in detail. This involves the unfolding of a flattened, prefolded section of carton

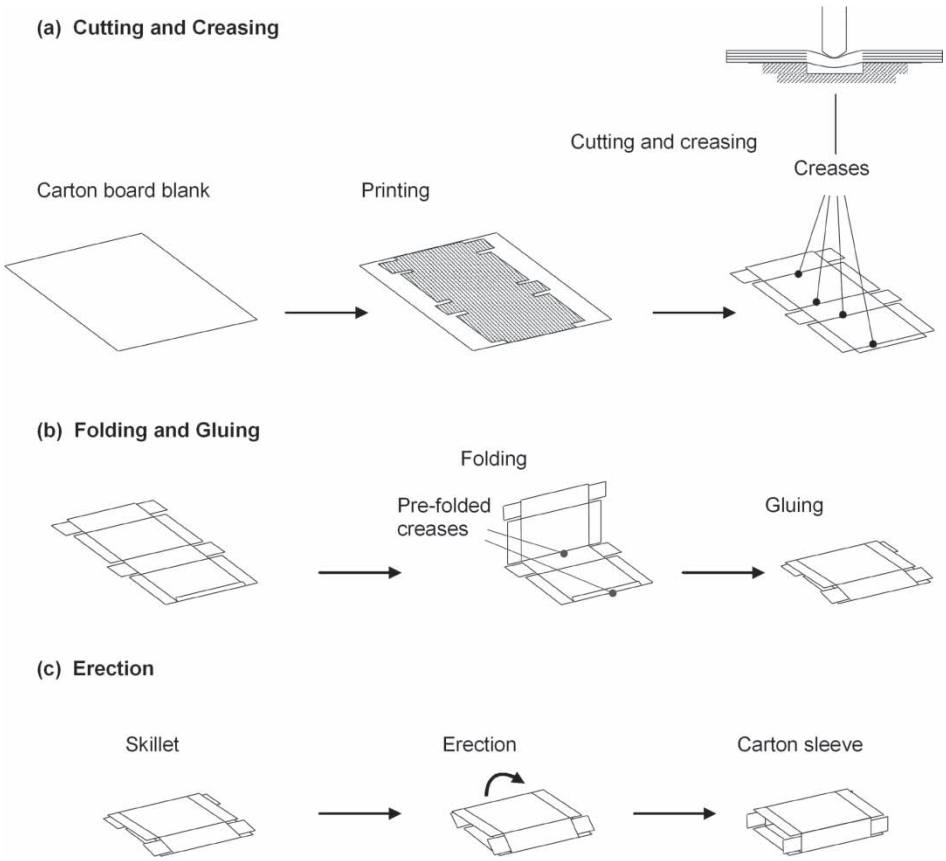

Fig. 1 Stages in the manufacture of a folding carton

board known as a 'skillet' into a sleeve. To make a skillet, a sheet of carton board is initially printed and then is cut and creased in one operation [Fig. 1(a)]. Creasing causes local delamination, which ensures that folding occurs at precisely the intended location. After creasing, the board is folded and glued along the overlap to form a sleeve. The finished skillet is then rolled flat before being stacked for space-saving transit. The skillet is stored in the flattened state before being erected into a carton. Erection is typically achieved by forcing one edge of the skillet against a fixed plate. Once the skillet has been erected, the contents are inserted and the final stages of conversion – flap closure and gluing – take place.

2.2 Modelling packaging material behaviour

The material used to make a folding carton is termed 'carton board' and is usually a 0.31–0.81 mm thick laminate consisting of three to five layers of paper [**1**]. The carton board is an orthotropic material [**16**]. This is because during its manufacture, the majority of the fibres orient themselves in a preferred direction, known as the machine direction (MD). The direction perpendicular to this is known as the cross direction (CD). Furthermore, the properties of the board in the thickness direction (ZD) differ from those of MD and CD because of its laminar construction. Considerable research effort has been taken with the aim of investigating the mechanical properties of the carton board. In-plane bending stiffness [**12**, **16**, **17**], properties in the thickness direction [**17**, **18**], and the effects of the creasing operation on board structure and folding behaviour [**6**, **19**, **20**] have all been studied. Research of this kind has led to a number of reliable standard tests, which are used by the carton and carton board industry to assess the material properties.

2.3 Crease folding

Although a simple linear material model is adequate to predict its response to small strains, at high levels of deformation, the behaviour of the carton board becomes non-linear. This is because stress in the thickness direction (ZD) is poorly resisted and tends to cause delamination. Deformation sufficient to permanently damage the interlaminar bonds occurs initially during the creasing operation. Further delamination followed by buckling of the individual plies then occurs in the creased zone as

it is folded. These creased zones and their interactions govern the behaviour of the cartons. It is, therefore, necessary to reliably model the crease behaviour in order to simulate the response of the skillet during processing.

2.4 Modelling crease behaviour

The response of the carton board to creasing and folding is difficult to model computationally because of the complex non-linear delamination buckling phenomena that occur. Several authors have attempted to create FE [**6**, **21**, **22**] and mathematical [**20**, **23**] models of crease folding behaviour. Recently, energy methods have also been used to model the crease-folding behaviour [**11**]. Although there have been several different approaches to the problem of simulating the behaviour of a single crease, there has been comparatively little work that applies and extends these approaches to consider a complete pack and its behaviour during processing. The interaction that takes place among the four creases and the skillet walls is fundamental to understanding and simulating the skillet erection process [**10**]. Of the work that has been undertaken, one study investigated the deformation response of a pack to static loading as would occur during palletized transit [**24**], and a simplified case of skillet erection has been created which considered erection by virtue of end-shortening [**10**].

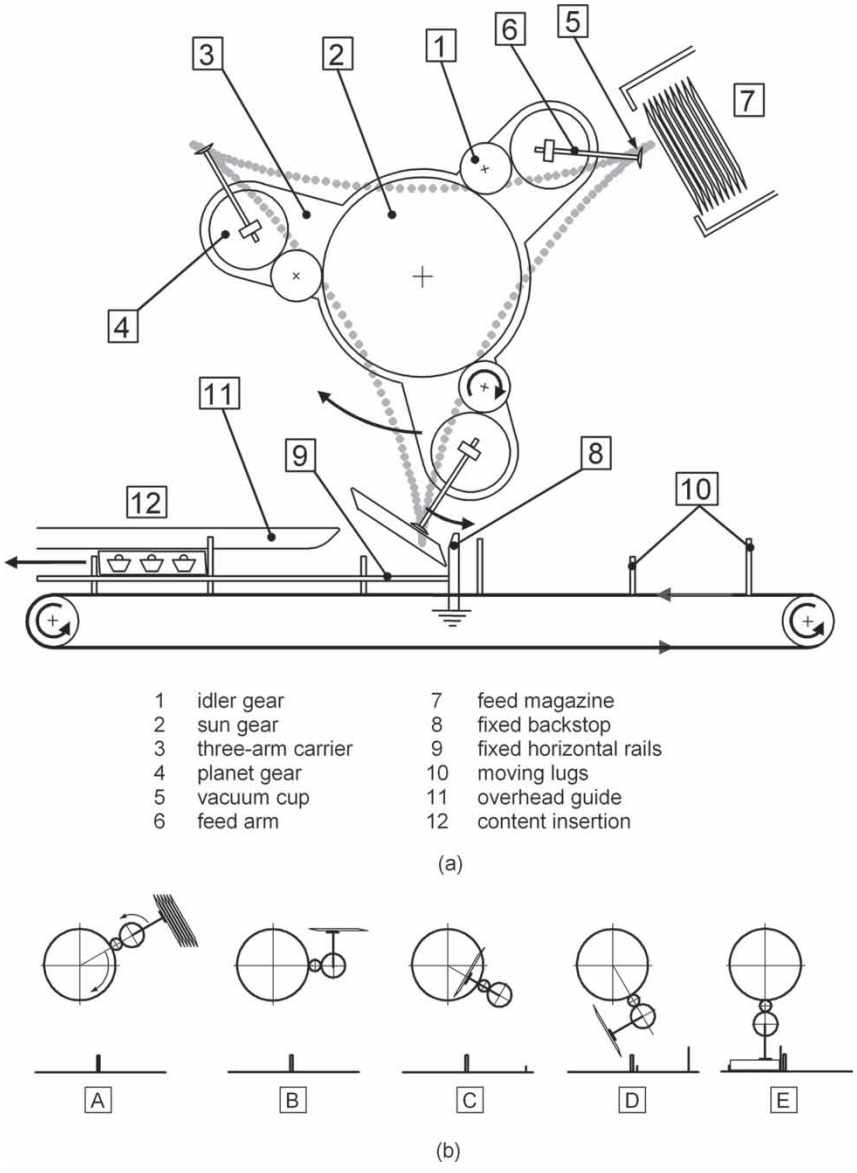

Fig. 2 (a) Schematic diagram of a three-station epicyclic skillet erection mechanism and (b) five-frame sequence illustrating the motion of the mechanism from pick-up of skillet (A) to erected carton (E)

2.5 Modelling interactions

In order to maximize the benefit of this work to the packaging industry, it is necessary to model, in addition to the creases and skillet structure itself, the material–machine interactions that occur during its processing. Effects that must be considered include the kinematics and phasing of the moving parts of the machine, the pick-up of the skillet from the feed magazine and its release into the conveyor system, and the friction and contact interactions that occur during collision with and sliding against the fixed and moving components of the packaging machine.

2.6 Skillet erection cycle

A common method of erecting a skillet is by using an epicyclic mechanism. A typical three-station configuration is shown in Fig. 2(a). This is capable of achieving production rates in excess of 200 cartons per minute (CPM). In the three-station mechanism, idler gears (1) rotate clockwise against a fixed sun gear (2) and this causes the three-arm carrier (3) to rotate clockwise, whereas the planet gears (4) revolve in the anticlockwise direction. The locus of movement of the vacuum cups (5) located at the end of the feed-arm (6) is illustrated in the figure by grey dots. Wider spaced dots indicate higher velocities. The kinematic properties of the epicylic mechanism are ideal for skillet picking and erecting, as the velocity of the vacuum cups is at a minimum at the two critical transfer points. In operation, a skillet is drawn from a feed magazine (7) and is held securely by the vacuum cups. It is then accelerated and rotated anticlockwise towards a fixed backstop (8). The leading edge of the skillet is forced into contact with the backstop by the movement of the feed-arm and this initiates the erection process. As the leading edge nears the fixed rails (9), it is approached by the moving lugs (10), which are attached to a chain drive. The impact with the moving lugs completes the erection process and when the feed-arm is at bottom-dead-centre, the vacuum to the cups is released. The erected carton then slides under the overhead guide (11) before being filled with product (12) and transported to further processes downstream. The operation is summarized in Fig. 2(b), which shows the skillet at different points in its travel.

2.7 Machine set-up

When setting-up a packaging machine for a particular carton, there are several parameters that directly affect the erection phase. A diagram highlighting these parameters can be seen in Fig. 3. Of the dimensions shown, the most important adjustments are thought to be the point of vacuum cup attachment on the skillet, d_v, the angle of the backstop, θ_b, and its position, d_b, with respect to the epicyclic mechanism. At present, the effects of these variables and how they relate to pack shape and size are not well understood and it is frequently necessary to use empirical methods to fine-tune machine performance for a particular pack. Although this has proved adequate up until now, the introduction of a more systematic approach is necessary to enable machinery manufacturers to consider the implications of thinner, lighter-weight boards during machine design and commissioning.

2.8 Process failure

The purpose of the epicyclic mechanism shown in Fig. 2 is to open up skillets into rectangular sleeves.

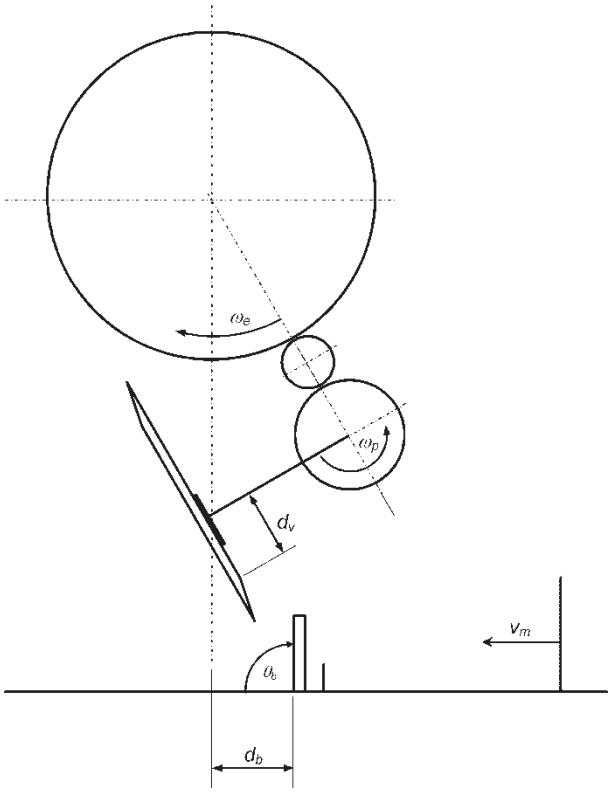

d_b backstop distance from epicyclic centre
d_v vacuum-cup distance from crease
θ_b backstop angle
ω_e epicyclic carrier angular velocity
ω_p epicyclic planet angular velocity
v_m moving lug velocity

Fig. 3 Schematic diagram highlighting key dimensions and velocities of the epicyclic mechanism

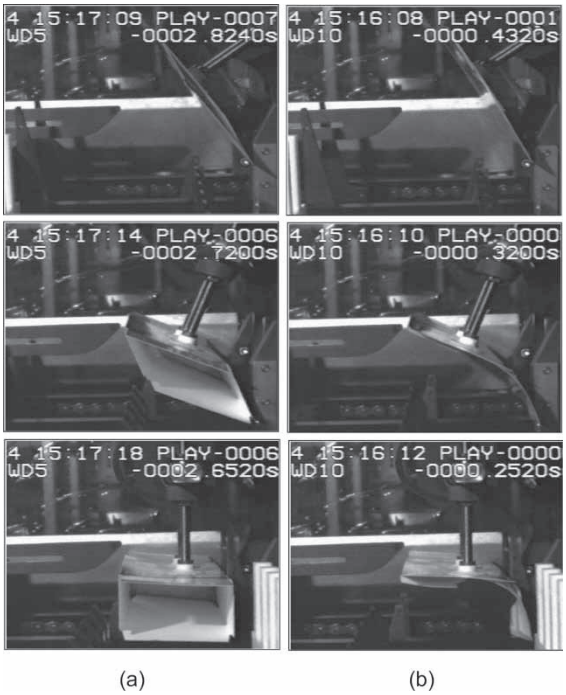

Fig. 4 Normal skillet erection (a) and buckling failure (b)

This is generally a reliable process but can fail and the reasons for this are not fully understood. During such a failure, the skillet walls effectively stick together instead of separating, which causes the structure to buckle. Several factors are thought to predispose a skillet to buckling. These include the initial opening of the walls, which is influenced by the spring-back in the prefolded creases, the stiffness of the board and creases in relation to the size of the skillet, and the position of the backstop. There is evidence to suggest that the cross-sectional shape of the skillet plays a role too, with the tendency to buckle increasing as the aspect ratio approaches 1:1. Figure 4(a) shows a skillet being erected normally at a production rate of 80 CPM, whereas a buckling failure captured at the same production rate is illustrated in Fig. 4(b).

3 METHODS

The model created in the present study was based upon the shape and mechanical properties of an actual carton whose dimensions are shown in Fig. 5. Mechanical testing was performed to determine the material properties of the wall sections and the folding/unfolding characteristics of the creased regions. This used techniques previously developed by the authors [**10**]. The model was created using ABAQUS/Standard 6.4 (ABAQUS Inc.) FE analysis software.

3.1 Wall elements

The carton board used in the skillet was a three-layer laminate. The material was modelled using overall properties for the laminate, which were obtained through mechanical testing following storage of at least 24 h in an atmosphere of 50 per cent relative humidity at 23°C. Three-point bending tests were performed in accordance with relevant standards [**25**] in order to obtain elastic moduli for the MD and CD. Three replicates of each test were performed in order to calculate mean values. The elastic modulus in the thickness direction was estimated using equation (1), according to the results of a previous

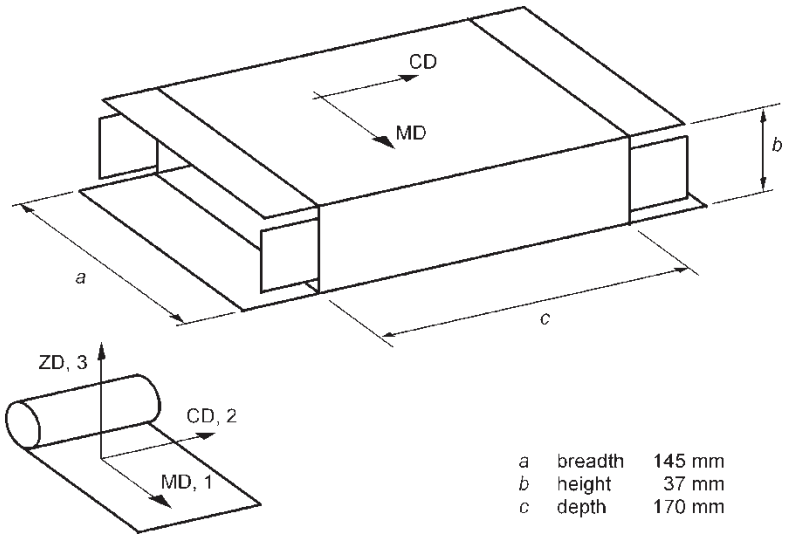

Fig. 5 Dimensions of the carton on which the FE model was based showing alignment of principal material axes

Table 1 Material properties for the carton material

Property	Print side convex	Print side concave
E_1 (MPa)	5430.4	5126.8
E_2 (MPa)	2507.1	2704.9
E_3 (MPa)	28.6	25.6
G_{12} (MPa)	1439.0	1452.3
G_{13} (MPa)	100.6	93.2
G_{23} (MPa)	71.6	77.3
ν_{12}	0.15	0.15
ν_{13}	0.008	0.008
ν_{23}	0.021	0.021
ν_{21}	0.32	0.32
ν_{31}	1.52	1.52
ν_{32}	1.84	1.84
μ_s	0.29	0.29
ρ (kg/m)^3	634.0	634.0
t (mm)	0.415	0.415

study [**26**]

$$E_3 = \frac{E_1}{190} \tag{1}$$

Shear modulus values were derived from elastic moduli using equation (2) as given in references [**24**] and [**26**]

$$G_{12} = 0.387\sqrt{E_1 E_2} \quad G_{13} = \frac{E_1}{54} \quad G_{23} = \frac{E_2}{35} \tag{2}$$

Owing to the difficulty of measuring Poisson's ratio, the values were those obtained in a previous study of carton board properties [**26**].

The coefficient of sliding friction between the printed side of the board and smooth stainless steel, and the board thickness were found in accordance with industry standards [**27**, **28**], respectively. These data together with the elastic moduli are summarized in Table 1.

In the ABAQUS model, the walls of the skillet were modelled as type S4R four-node shell elements with reduced integration. In order to account for the anisotropy of the carton walls, an orthotropic material model of the form shown in equation (3) was specified with principal axes, as illustrated in Fig. 5. Material properties for the two cases considered in Table 1 were assigned according to the direction of bending of the walls. Plasticity and non-linear effects were not incorporated into the orthotropic material model for the wall elements, as the strain levels experienced during bending deformation were within the linear portion of the stress–strain characteristic for carton board. Although delamination and yielding do take place during folding of the creases, this behaviour was accounted for by the non-linear response of the hinge elements used to represent these regions (section 3.2). A summary of the material models and boundary conditions applied to the model is provided in Table 2

$$\begin{Bmatrix} \varepsilon_{11} \\ \varepsilon_{22} \\ \varepsilon_{33} \\ \gamma_{12} \\ \gamma_{13} \\ \gamma_{23} \end{Bmatrix} = \begin{bmatrix} \frac{1}{E_1} & \frac{-\nu_{21}}{E_2} & \frac{-\nu_{31}}{E_3} & 0 & 0 & 0 \\ \frac{-\nu_{12}}{E_1} & \frac{1}{E_2} & \frac{-\nu_{32}}{E_3} & 0 & 0 & 0 \\ \frac{-\nu_{13}}{E_1} & \frac{-\nu_{23}}{E_2} & \frac{1}{E_3} & 0 & 0 & 0 \\ 0 & 0 & 0 & \frac{1}{G_{12}} & 0 & 0 \\ 0 & 0 & 0 & 0 & \frac{1}{G_{13}} & 0 \\ 0 & 0 & 0 & 0 & 0 & \frac{1}{G_{23}} \end{bmatrix} \times \begin{Bmatrix} \sigma_{11} \\ \sigma_{22} \\ \sigma_{33} \\ \sigma_{12} \\ \sigma_{13} \\ \sigma_{23} \end{Bmatrix} \tag{3}$$

3.2 Connector elements

In this study, the crease regions were modelled as hinge-type connector elements incorporating non-linear torsional springs. As these elements connect two individual nodes only, further constraints were

Table 2 Summary of material models and boundary conditions applied to the various parts of the model

Part	Material/connector model	Boundary conditions/constraints
Backstop	Discrete rigid	U1, U2, U3, R1, R2, R3 = 0
Horizontal rail	Discrete rigid	U1, U2, U3, R1, R2, R3 = 0
Moving lug	Discrete rigid	U2, U3, R1, R2, R3 = 0, V1 = v_m
Feed arm	Discrete rigid	U1, U2, U3, R1, R3 = 0, VR2 = ω_p
Arm carrier	Discrete rigid	U1, U2, U3, R1, R3 = 0, VR2 = ω_e
Vacuum cup	Isotropic, linear elastic	All d.o.f. on rear surface fixed w.r.t. feed arm (kinematic constraint)
Carton walls	Orthotropic, linear elastic	Adjacent walls connected by hinge elements at corners. U1, U3, R2 on wall edge parallel to 2 axis fixed w.r.t. wall corner (kinematic constraint)
Carton creases	Hinge elements, user-defined torsional stiffness	

applied to the edges adjoining the corners of the walls so as to distribute the kinematic and kinetic behaviours along the full depth of each crease.

3.3 Connector behaviour

Mechanical testing of the creased regions from a skillet was performed to define the response of the hinge connector elements. Sections of skillet 80 mm wide from all four creases were placed into a specially designed crease-testing apparatus [Fig. 6(a)] in order to determine the relationship between torque and angular displacements. Mean values were taken from three replicate tests to find the overall characteristic. In order to account for frictional losses in the apparatus, testing was first performed without a sample in place and the resulting offset was subtracted from all recorded data. Polynomial curves were fitted through the set of mean data points and were used to generate tabular data for the ABAQUS model.

Mechanical testing revealed three distinct characteristics among the creased regions [Fig. 6(b)]. Although the two unfolding creases shared a common response, there was a significant difference in the behaviour of the two folding creases. This may be explained by the fact that one of these creases lies immediately adjacent to the glued seam of the skillet.

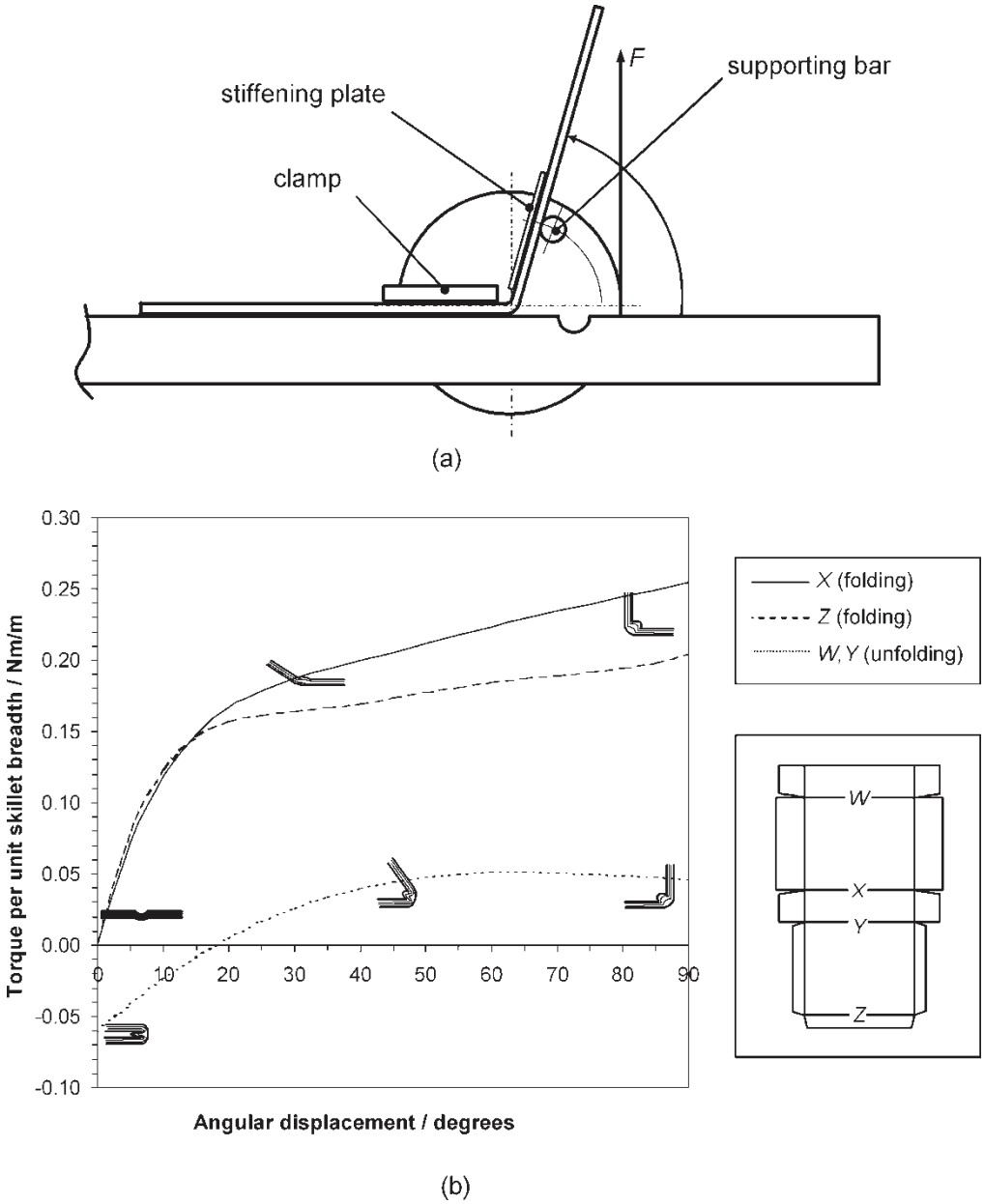

Fig. 6 (a) Apparatus used to perform crease tests and rotational opening and (b) torque-angle relation for unfolding of pre-folded creases and folding of unfolded creases

During its manufacture, the entire skillet is rolled flat once the seam overlap has been glued. As there is a triple thickness of the carton board at the seam and only a double thickness elsewhere, the compression applied during the rolling process is highest in this region. The high compressive force can alter the mechanical properties of the carton board in crease *Z* [inset, Fig. 6(b)] which may explain the attenuated torque response observed in this crease. For the unfolding crease property, the torque values were initially negative due to spring-back resulting from compression of the crease bead. In the FE model, the spring-back was balanced by the resistance of the two unfolded creases. This resulted in an equilibrium state in which an initial separation between the long walls was created. This initial opening is termed 'plim' by the carton industry.

3.4 Model validation against experimental opening

A rotational opening test was performed on an 80 mm wide section of a skillet using the crease-testing apparatus but without the stiffening strip. The test was simulated in ABAQUS and the resulting pattern of deformation was compared with the video footage of the experimental case. Figure 7(a) shows the deformed shape of the skillet, whereas Fig. 7(b) shows these images overlaid on frames from a video of the skillet opening. For quantitative evaluation of the experimental results, the torque required to drive the supporting bar was investigated. Figure 8(a) shows a comparison of the experimental versus theoretical torque requirements for opening the skillet, whereas the energy input to the skillet during opening is shown in Fig. 8(b). This is discussed in section 4.

3.5 Simulation of mechanised erection process

The epicyclic mechanism commonly used to erect skillets was modelled using measurements taken from an industrial packaging machine. A schematic diagram of the mechanism is shown in Fig. 3. The feed-arm was modelled in ABAQUS as a rigid shaft attached at one end to a rotating hinge connector and at the other to a 1 mm thick block of deformable rubber with an elastic modulus of 20 MPa. Kinematic

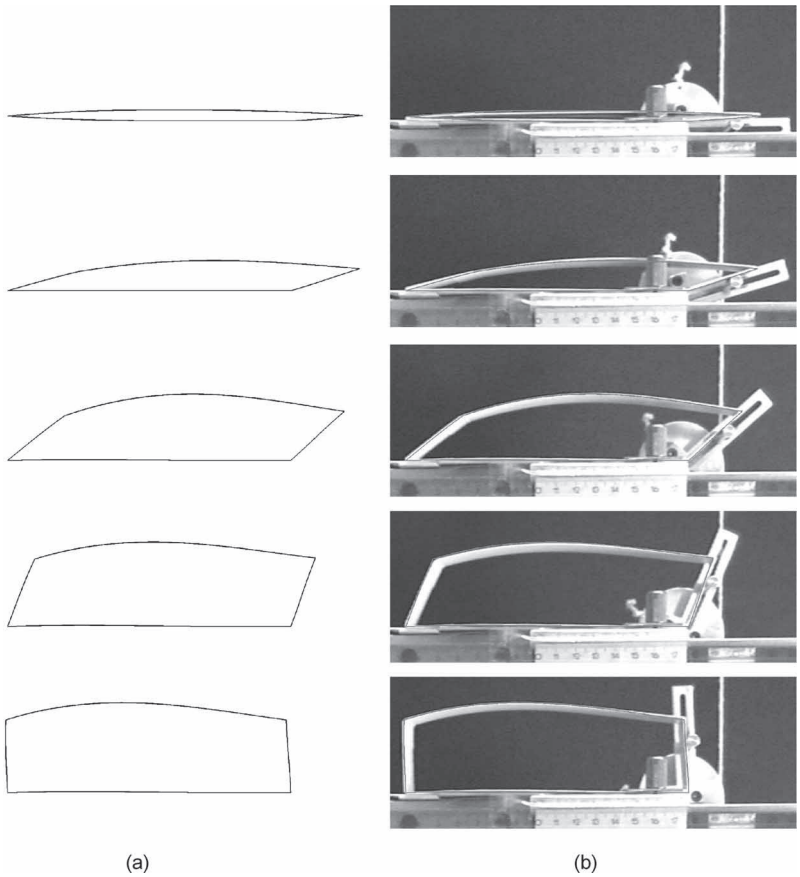

Fig. 7 Visual comparison of deformed shaped during rotational opening of the skillet: (a) predicted deformation and (b) images of actual deformation with predicted results superimposed

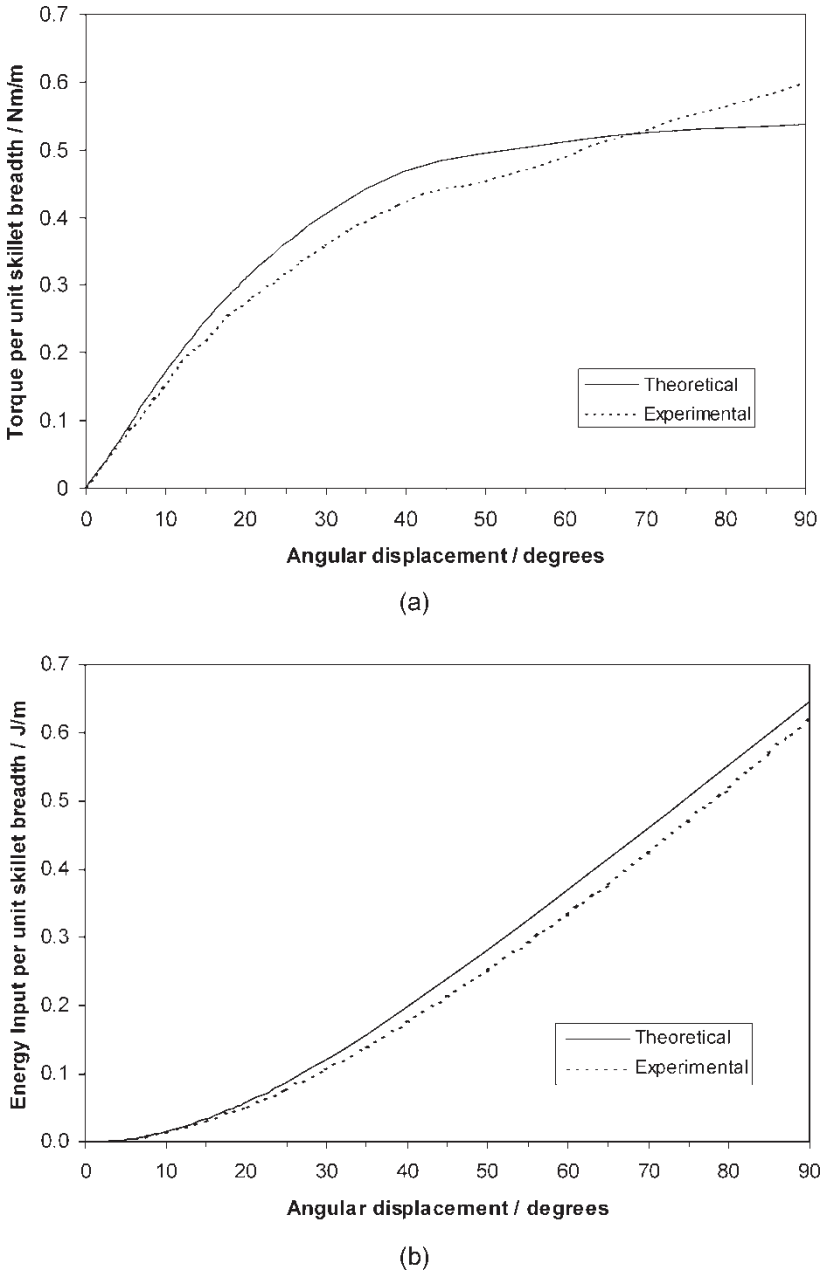

Fig. 8 (a) Graph comparing the torque required to open the skillet by rotating one wall using the crease-folding apparatus for the theoretical and experimental case and (b) graph comparing the work done in opening the skillet

constraints were placed on the non-skillet-contacting surface of the rubber block in order to provide a rigid backing. Deformation of the block in the thickness direction was unconstrained. The skillet was held against the rubber block by a pressure load of 10 kPa applied to the underside of the upper wall. A 'rough' (i.e. no slip) contact formulation was applied for this interaction [**29**]. The vacuum pressure held the skillet in place during erection and transfer to the moving lugs and no additional constraints were imposed. The motion sequence considered by the simulation represents the portion of the cycle illustrated in frames D to E of Fig. 2(b). A schematic diagram outlining the sequence of events, boundary conditions, loads, and interactions taking place during the simulation is shown in Fig. 9.

Contact interactions were applied between the walls of the skillet and the fixed backstop, the moving lugs, and the fixed horizontal rails of the packaging machine. Contact was based upon master/slave interactions, with the skillet walls defined as slave surfaces in all cases. A 'hard' pressure overclosure formulation was used and penalty-type friction was applied for all interactions in which

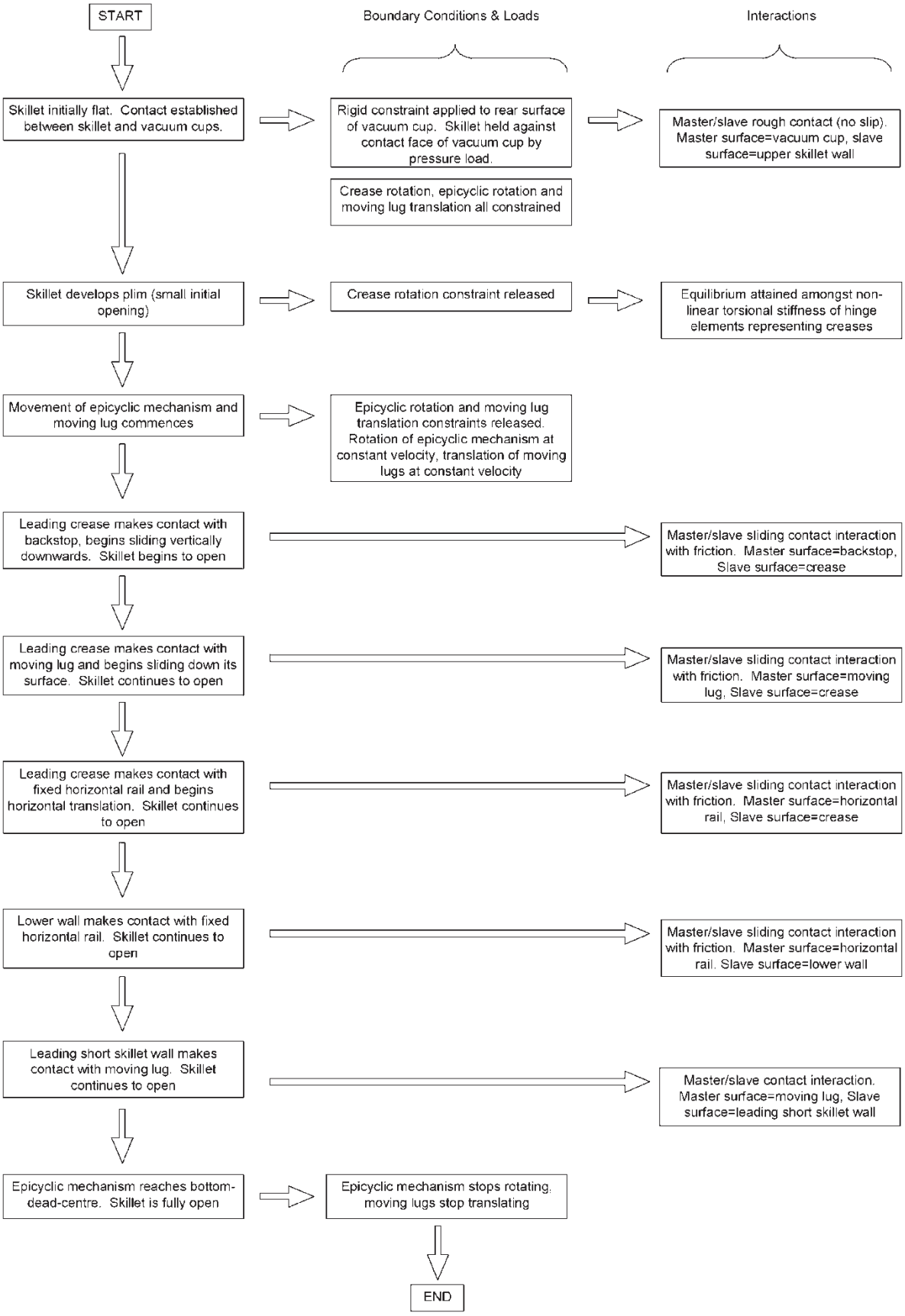

Fig. 9 Schematic diagram showing key stages, boundary conditions, loads, and interactions of the simulation of skillet erection within the packaging machine

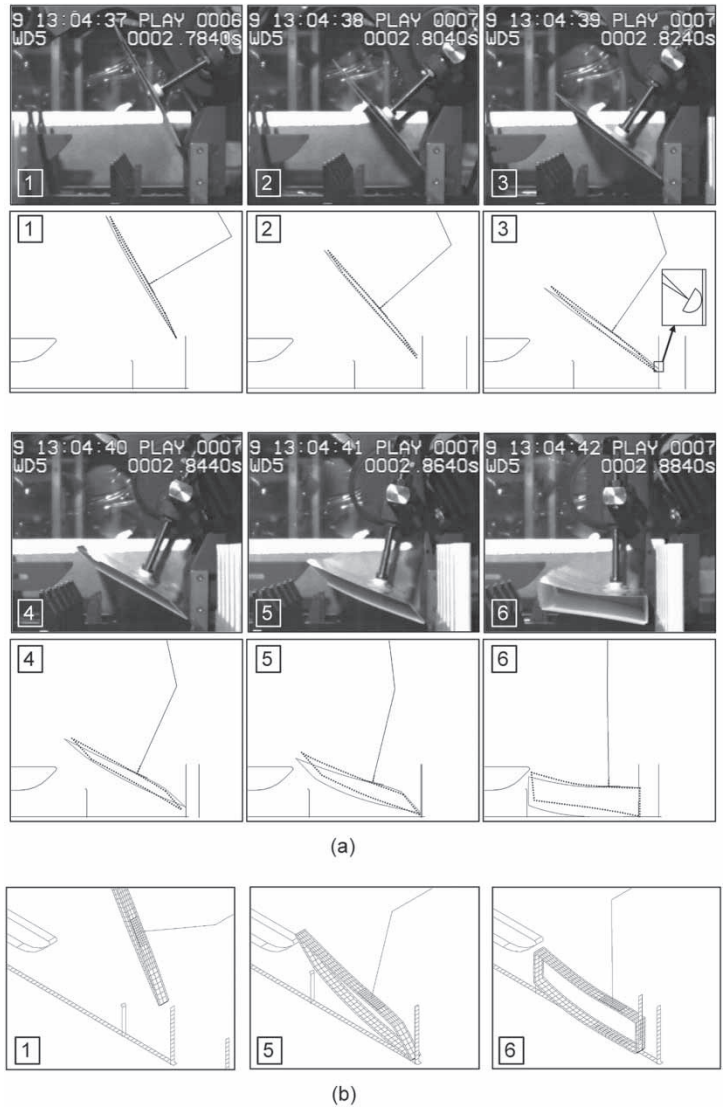

Fig. 10 (a) Comparing the pattern of deformation predicted by the FE model with the physical system. The actual deformation is superimposed with a dotted line on the simulation images and (b) isometric view of three stages in the simulation

significant relative movement between surfaces occurred [**29**]. A semicylindrical surface 10 mm in length and having a radius equal to the board thickness was attached to one edge of the lower wall in order to simulate crease contact with the backstop [inset, Fig. 10(a), frame 3].

In order to reduce the number of elements required, the simulation considered a 10 mm deep section of the skillet depicted in Fig. 5. That is to say dimension *c* on the figure was set to 10 mm. However, it was necessary to consider in addition the stiffening effect of the flaps adjoining the walls of the skillet. Therefore, strips of material having depth dimensions scaled appropriately were joined to the edges of the skillet section to represent the flaps. Crease folding and unfolding stiffness was assumed to be directly proportional to the length of crease (i.e. dimension *c* in Fig. 5) and so the magnitudes were adjusted to give the response expected of a carton 10 mm deep.

4 RESULTS

This section first describes the results of the validation study by rotational opening before considering the results of the simulation of carton behaviour within the packaging machine.

4.1 Validation of pack model

The purpose of the rotational opening test was to validate the pack model qualitatively in terms of the pattern of deformation of the walls and

quantitatively by considering the relationship between opening torque and angular displacement. The sequence of images in Fig. 7 shows very good agreement between the model and the experimental case over the full range of angular displacement. The quantitative results shown in Fig. 8(a) suggest a good match also in terms of the opening torque requirement. However, the line for the theoretical case is initially steeper than the experimental case and at 30° of opening the predicted torque value is 12.8 per cent higher than the experimental result. The theoretical curve gradually flattens out beyond 40°, whereas the experimental data indicate the stiffness is approximately constant in this region. At the fully open position, the predicted result is 10.2 per cent lower than the experimental value. The absolute error on the predicted results, averaged at 10° increments from 10° to 90° of opening, is 9.3 per cent. The effect of the stiffness discrepancies on the work done in opening the skillet was found by integrating the torque–angle relations. These results are shown in Fig. 8(b). The FE simulation was found to slightly over-estimate the energy requirement. At the fully open position, the error on the predicted results was found to be +5.1 per cent. Considering the analysis involves the simultaneous interaction of the four creases with the four walls, the qualitative match to experimental results is very good and the errors associated with the quantitative results are relatively small.

4.2 Simulation of pack processing

Figure 10(a) shows the pattern of deformation in the skillet during the simulated erection process against frames from high-speed video footage of an actual epicyclic mechanism running at a typical production rate of 150 CPM. An isometric view of three stages in the sequence is shown in Fig. 10(b).

In general, there is a good agreement between the model and the physical system. The main difference is that the upper wall of the skillet remains perpendicular to the feed-arm in the predicted results, yet is rotated clockwise slightly in the physical system. The maximum angular error (measured at the point of vacuum cup attachment) of 7.0° occurs in frame 5. This results in an error of 10.6 mm on the location of the trailing crease. It is likely that the rotational error is a consequence of air resistance, which was not modelled in the FE simulation. Furthermore, in frame 6 of Fig. 10(a), the lower wall of the model bows slightly in the opposite direction to the real skillet. This may be because in the physical system, the trailing edge of the skillet fouled the tip of the overhead guide, thereby compressing the carton in the breadth direction, and causing an upwards bowing of the lower wall. In the ABAQUS model, the overhead guide was positioned to allow a small clearance between its tip and the trailing edge of the skillet.

5 DISCUSSION

The requirement of the packaging industry under recent EU packaging waste legislation to use thinner, lighter-weight materials has stimulated demand for greater understanding of the processes involved in packaging operations. The trial and error approach to machine set-up and design used at present is both costly and not sustainable in the long term. In order to overcome these issues, it is necessary to develop an understanding of the behaviour of the pack and the key machine–material interactions that occur during processing.

Although a simplified computer model of a skillet in isolation has previously been created [**10**], the present study attempts to simulate the behaviour of the skillet within the mechanical processing environment. In order to achieve this, a system model which incorporates skillet, creases, interactions, and key machine elements was created. This model was initially validated against experimental results and showed good qualitative agreement with observed deformation behaviour over the full range of opening. Furthermore, the predicted energy requirement for this operation was within 6 per cent of the actual value. When extended to a simulation of carton erection in a packaging machine, the deformation predicted by the model showed maximum positional and angular errors of 10 mm and 7° respectively, compared with actual behaviour during processing.

The model enables the effect of variations in machine set-up, material properties, and pack geometry on the normal carton erection process to be investigated. For example, if a new pack size is specified then the simulation can be used to confirm whether the skillet will erect correctly within the limits of adjustability of the machine and if so, recommended settings together with tolerance ranges can be obtained. Furthermore, the simulation can also be used to investigate the effects of modifying the kinematics of the erection process. For example, the effect of changing the dimensions or relative velocities of the epicyclic mechanism components or its point of attachment on the skillet can easily be simulated. By monitoring the reaction forces occurring at the machine–material interactions, the model can also allow settings to be adjusted for minimum contact force which may help reduce tooling wear.

The objective of the work presented here was to simulate the case of normal skillet erection within a packaging machine. However, if additional factors such as aerodynamic effects are included, then it will in addition be possible to simulate the case of process failure. Design guidelines can then be produced which relate desired production rates to carton geometry, material properties, and machine settings. Such information will be valuable for carton producers, packaging machine manufacturers, and carton end-users.

6 CONCLUSION

In order to improve the design and operation of high speed production machinery, it is becoming increasingly necessary to understand the key machine–material interactions that take place. This is a fundamental requirement for the manufacturing industry in general, but is specifically important for the packaging industry. To address the need for greater understanding of complex packing operations, a simulation of the behaviour of folded cartons during processing within an epicyclic erection mechanism has been created. The fundamental contribution of this work is that the simulation considers both the pack itself and the interaction of the pack with the packaging machine. In producing the FE model, a method for acquiring and representing the non-linear behaviour of the creased regions and their interaction within the structure of the skillet was successfully validated. An orthotropic material model was applied to the skillet walls with elastic moduli obtained through mechanical testing. The pattern of deformation of the resulting carton structure and the opening force characteristic both closely matched experimental results. In simulating the machine–material interactions during processing of the pack, the performance of the model in response to large displacements, multiple concurrent interactions, and large deformations compared well with observed carton behaviour. It may, therefore, be concluded that the method outlined in this paper is suitable for modelling the behaviour of folding cartons during normal erection.

ACKNOWLEDGEMENTS

The work reported in this paper has been undertaken as of the EPSRC Innovative Manufacturing Research Centre at the University of Bath (grant reference GR/R67507/0). The work has also been supported by a number of industrial companies and engineers. The authors gratefully acknowledge this support and express their thanks for the advice and support of all concerned.

REFERENCES

1 **Packaging Federation.** Packaging in the 3rd millennium: competitiveness study for the packaging industry in the UK, 20 May 2005, available from http://www.packagingfedn.co.uk/news/fed_arch/mainreport.pdf.
2 **Pro Carton Europe.** Carton industry basic information, 1 June 2005, available from http://www.procarton.com/facts/basicinformation.php.
3 **Office for National Statistics.** Product sales and trade: cartons, boxes, cases & other containers. PRA21219, 2000, available from http://www.statistics.gov.uk/downloads/theme_commerce/PRA-20000/PRA21219_20000.pdf, accessed 3 June 2005.
4 **European Union Directive.** European packaging and packaging waste directive 2004/12/EC of 11 February 2004 amending 94/62/EC11, 2004.
5 **Emslie, A. G.** and **Brenneman, R. S.** A theoretical and experimental study of the scoring and bending of boxboard. *Tappi*, 1967, **50**, 289–297.
6 **Carlsson, L., Fellers, C.,** and **Westerlind, B.** Finite element analysis of the creasing and bending of paper. *Svensk Papperstidning*, 1982, **15**, 121–126.
7 **Steenberg, B., Kubat, J., Martin-Löf, S.,** and **Rudström, L.** Competition in rigid packaging materials. *Svensk Papperstidning*, 1970, **73**, 77–91.
8 **Cavlin, S. I.** The unique convertibility of paperboard. *Packag. Technol. Sci.*, 1988, **1**, 77–92.
9 **Hanlon, J. F., Kelsey, R. J.,** and **Forcinio, H. E.** Folding cartons and set-up boxes. In *Handbook of package engineering*, 1998 (Technomic Publishing Company Inc., Lancaster, Pennsylvania).
10 **Hicks, B. J., Berry, C., Mullineux, G., McPherson, C. J.,** and **Medland, A. J.** An energy-based approach for modelling the behaviour of packaging material during processing. *Proc. Instn Mech. Engrs, Part C: J. Mechanical Engineering Science*, 2004, **218**, 105–118.
11 **Hicks, B. J., Mullineux, G., Berry, C., McPherson, C. J.,** and **Medland, A. J.** Energy method for modelling delamination buckling in geometrically constrained systems. *Proc. Instn Mech. Engrs, Part C: J. Mechanical Engineering Science*, 2003, **217**, 1015–1026.
12 **Carlsson, L.** and **Fellers, C.** Flexural stiffness of multiply paperboard. *Fibre Sci. Technol.*, 1980, **13**, 213–223.
13 **Ramasubramanian, M. K.** and **Muthuraman, K.** A computational mechanics model for the brim forming process in paperboard container manufacturing. *J. Manuf. Sci. Eng., Trans. ASME*, 2003, **125**, 476–483.
14 **Babini, A., Borsari, R., Dughiero, F., Fontanini, A.,** and **Forzan, M.** 3D FEM models for numerical simulation of induction sealing of packaging material. *COMPEL, Int. J. Comput. Math. Electr. Electron. Eng.*, 2003, **22**, 170–180.
15 **Yang, Z. J., Harkin-Jones, E., Menary, G.H.,** and **Armstrong, C. G.** A non-isothermal finite element model for injection stretch-blow molding of PET bottles with parametric studies. *Polym. Eng. Sci.*, 2004, **44**, 1379–1390.
16 **Edholm, B.** Bending stiffness loss of paperboard at conversion – predicting the bending ability of paperboard. *Packag. Technol. Sci.*, 1998, **11**, 131–140.

17 **Fellers, C.** Bending stiffness of paper and paperboard – a round robin study. *Nord. Pulp Paper Res. J.*, 1997, **12**, 42–45.

18 **Stenberg, N., Fellers, C.,** and **Östlund, S.** Plasticity in the thickness direction of paperboard under combined shear and normal loading. *Trans. ASME, J. Eng. Mater. Technol.*, 2001, **123**, 184–190.

19 **Nagasawa, S., Fukazawa, Y., Yamaguchi, T., Tsukatani, S.,** and **Katayama, I.** Effect of crease depth and crease deviation on folding deformation characteristics of coated paperboard. *J. Mater. Process. Technol.*, 2003, **140**, 157–162.

20 **Carlsson, L., De Ruvo, A.,** and **Fellers, C.** Bending properties of creased zones of paperboard related to interlaminar defects. *J. Mater. Sci.*, 1983, **18**, 1365–1373.

21 **Gilchrist, A. C., Suhling, J. C.,** and **Urbanik, T. J.** Nonlinear finite element modeling of corrugated board. *Mech. Cellulosic Mater.*, 1999, **231**, 101–106.

22 **Sinha, S. K.** and **Perkins, R. W., Jr.** A micromechanics constitutive model for use in finite element analysis. *Mech. Cellulosic Mater.*, 1995, **60**, 69–89.

23 **Xia, Q. X. S., Boyce, M. C.,** and **Parks, D. M.** A constitutive model for the anisotropic elastic–plastic deformation of paper and paperboard. *Int. J. Solids Struct.*, 2002, **39**, 4053–4071.

24 **Beldie, L., Sandberg, G.,** and **Sandberg, L.** Paperboard packages exposed to static loads – finite element modelling and experiments. *Packag. Technol. Sci.*, 2001, **14**, 171–178.

25 **British Standards.** *Determination of the bending stiffness of paper and board by static methods.* BS7424, 1991.

26 **Mann, R. W., Baum, G. A.,** and **Habeger, C. C.** Determination of all nine orthotropic elastic constants for machine-made paper. *Tappi*, 1980, **63**, 163–166.

27 **American Society for Testing and Materials.** *Standard test method for static and kinetic coefficients of friction of plastic and film sheeting.* ASTM D1894, 2001.

28 **British Standards.** *Method for determination of thickness and apparent bulk density or apparent sheet density of paper and board.* BS EN 20534, 1993.

29 ABAQUS/Standard version 6.4 User's Manual, *Prescribed conditions, constraints and interactions*, 2003, vol. V (Hibbit, Karlsson & Sorensen, Inc., USA).

BIBLIOGRAPHY

Baum, G. A., Brennan, D. C., and **Habeger, C. C.** Orthotropic elastic constants of paper. *Tappi*, 1981, **64**, 97–101.

Stenberg, N. and **Fellers, C.** Out-of-plane Poisson's ratios of paper and paperboard. *Nord. Pulp Paper Res. J.*, 2002, **17**, 387–394.

APPENDIX

Notation

a	carton breadth
b	carton height
c	carton depth
d_b	horizontal distance between backstop and centre-line of epicyclic mechanism
d_v	distance between centre of vacuum cup and crease
E_1	modulus of elasticity in the machine direction (MD) (axis 1)
E_2	modulus of elasticity in the cross direction (CD) (axis 2)
E_3	modulus of elasticity in the thickness direction (ZD) (axis 3)
G_{12}	shear modulus in the MD–CD plane
G_{13}	shear modulus in the MD–ZD plane
G_{23}	shear modulus in the CD–ZD plane
t	thickness of the carton board
θ_b	backstop angle
μ_s	coefficient of sliding friction
v_m	moving lug velocity
ν_{12}, ν_{21}	Poisson's ratios in the MD–CD plane
ν_{13}, ν_{31}	Poisson's ratios in the MD–ZD plane
ν_{23}, ν_{32}	Poisson's ratios in the CD–ZD plane
ρ	density of the carton board
ω_e	epicyclic carrier angular velocity
ω_p	epicyclic planet angular velocity